JOURNAL OF APPLIED ELECTROCHEMISTRY 26 (1996) 493–502

A phenomenological approach to hydrous nickel oxide electrodes prepared by applying periodic potential routines

A. VISINTIN, W. E. TRIACA, A. J. ARVIA

Instituto de Investigaciones Fisicoquímicas Teóricas y Aplicadas, INIFTA, Facultad de Ciencias Exactas, Universidad Nacional de La Plata, Casilla de Correo 16, Sucursal 4, (1900) La Plata, Argentina

Received 20 June 1995; revised 9 October 1995

The characteristics of hydrous nickel oxide layers formed by the application of a fast periodic square-wave potential routine to a polycrystalline nickel electrode in alkaline solutions of different composition have been studied. The charging/discharging properties of the electroformed oxide layers were derived from voltammetry. Infrared spectroscopy data indicated that the nickel oxide layers resulting from vacuum drying at 100 °C consisted of a mixture of Ni(II) and Ni(III) oxides, the Ni(II)/Ni(III) ratio depending on the characteristics of the potential routine. X-ray analysis data and SEM micrographs showed the amorphous nature of the thick hydrous nickel hydroxide films produced by the above mentioned procedure. A correlation between the properties of the nickel oxide layers and their electrochemical response in alkaline solution has been advanced.

1. Introduction

A number of procedures have been established for the preparation of metal oxide electrodes with outstanding electrocatalytic properties [1–6], particularly in relation to their reversible behaviour and charge storage capacity. One of these procedures is based upon the application of a well-defined periodic potential routine to a metal electrode in an aqueous electrolyte solution covering a potential range in which different oxidation states of the metal [4] are involved. Metal oxide layers produced either in acid or alkaline solution by using a periodic potential routine are generally better described as hydrous metal oxide layers [2–4] involving a much complex structure than that of simple metal oxide electrodes [3, 5]. Thick cobalt oxide electrodes were produced in this way by applying a repetitive square-wave potential (SWP) routine to a piece of cobalt immersed in alkaline solution [6]. These hydrous cobalt oxide electrodes can be considered as precursors of high surface area Co_3O_4 spinel electrodes which exhibit a high electrocatalytic activity for the oxygen evolution reaction (OER) in alkaline solution [6–8].

The electrochemical properties of hydrous metal oxide electrodes are known to depend on the potential routine used in the preparation procedure, the solution composition, the stirring condition and temperature [3–8]. From the practical standpoint, the stability of this type of electrode, either under open circuit or applied potential conditions, is extremely important.

A renewed interest in the preparation of nickel hydroxide electrodes with either a high charge storage capacity or high electrocatalytic activity has been recently manifested [9]. It has focused mainly on their use in batteries, such as Ni–Cd, Ni–Fe, Ni–Zn, Ni–H_2, and Ni-metal hydride batteries [10–12], microelectrochemical devices [13], photoelectrochemical cells [14], organic electrosynthesis [15] and water electrolysis [16]. The performance of conventionally prepared nickel hydroxide electrodes is largely disturbed by side reactions such as the conversion reactions of α-$Ni(OH)_2$ into β-$Ni(OH)_2$, and that of the β-NiOOH into γ-NiOOH [17–20], yielding products of lower charge storage capacity. These facts make it interesting to attempt to evaluate to what extent these detrimental processes will also appear at those hydrous nickel oxide electrodes prepared by means of the potential cycling technique [5].

Following preceding investigations [19, 20], this work provides a phenomenological approach to the stability and electrocatalytic activity of hydrous nickel oxide electrodes formed in alkaline solution by using a SWP routine, with special attention being paid to the characteristics of the periodic potential routine, the solution composition, and temperature.

2. Experimental details

Runs were made in a conventional Pyrex glass electrochemical cell with a nickel working electrode (WE), a large surface area platinum as counter electrode, and a reversible hydrogen electrode (RHE) as reference. Potentials in the text are given on the RHE scale. Each WE was made from a nickel wire 0.15–0.35 cm^2 in geometric area (Johnson Matthey Chem. specpure quality), which was cleaned in 1 : 1 H_2SO_4 : H_2O solution, repeatedly rinsed with triply distilled water, then immersed in aqueous

0021-891X

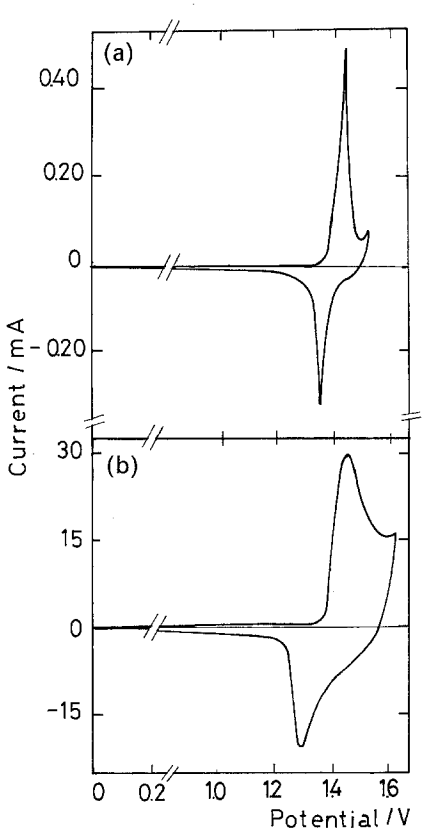

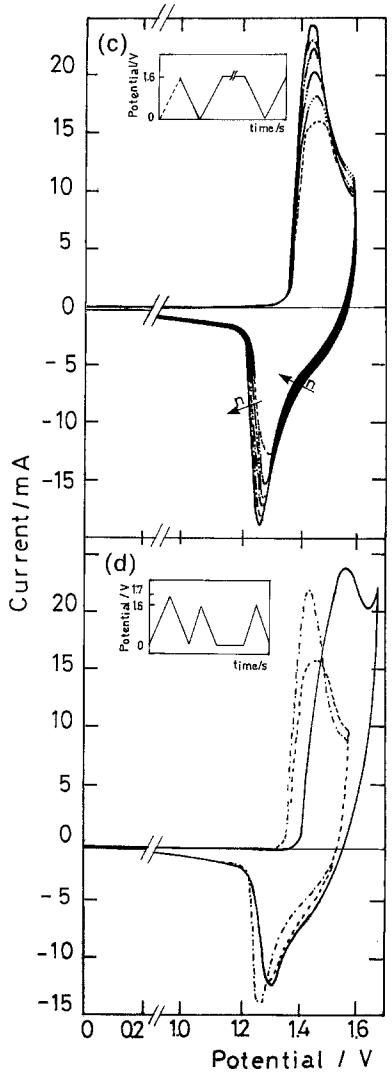

Fig. 1. Voltammograms run at $0.1\,V\,s^{-1}$ in 1 M NaOH, 30 °C. (a) untreated polycrystalline nickel WE (blank). (b) The same electrode after a 30 s SWP treatment ($E_l = -1.0\,V$, $E_u = 1.0\,V$, $f = 2\,kHz$. (c) Voltammograms run immediately after a 30 s SWP treatment ($E_l = -1.2\,V$, $E_u = 1.0\,V$, $f = 2\,kHz$) followed by a potential holding at 1.6 V for t_p: (- - -) 0 s; (– · · · · –) 15 s, (– · · · –)30 s, (– · · –) 45 s, (– · –) 60 s, (——) 150 s. (d) Voltammograms run immediately after a 30 s SWP treatment ($E_l = -1.2\,V$, $E_u = 1.0\,V$, $f = 2\,kHz$) followed by one ORC until 1.7 V (——), a second ORC until 1.6 V (——), and one ORC after a 50 s potential holding at 0 V (– · –).

x M NaOH ($x = 0.1$, 1 and 3), and finally subjected to a potential cycling at $0.1\,V\,s^{-1}$ between 0.05 and 1.55 V for 15 min.

Symmetric and asymmetric SWP routines were applied to the WE by adequately changing the upper (E_u) and lower (E_l) potential limits, the frequency (f), the half-period for the upper (τ_u) and the lower (τ_l) potential limit, and the SWP duration (t) in order to grow nickel oxide layers of different thicknesses. To determine the optimal conditions for producing the most efficient growth of the nickel oxide layer, the SWP routine characteristics were varied in the following ranges: $-2.0\,V \leqslant E_l \leqslant -0.40\,V$; $0.40\,V \leqslant E_u \leqslant 2.0\,V$; $0.1\,kHz \leqslant f \leqslant 3\,kHz$, and $0.3 \leqslant \tau_u/\tau_l \leqslant 2.3$. Runs were performed in the range 0 to 90 °C. Further details about the application of this technique have been given elsewhere [4, 5].

Each electrochemical run comprised the formation of the nickel oxide electrode by the application of the SWP to the WE immersed in aqueous NaOH. The WE was then subjected to an oxidation–reduction cycling (ORC) between 0.05 and 1.55 V at $0.1\,V\,s^{-1}$ for about 15 min to attain a stabilized voltammogram. The relative increase (R) in the Ni(III) voltammetric electroreduction charge (Q_r) was evaluated from the following ratio:

$$R = \frac{(Q_r)_a}{(Q_r)_b} \tag{1}$$

where $(Q_r)_b$ and $(Q_r)_a$ denote the Ni(III) voltammetric electroreduction charge before and after the SWP treatment, respectively, as estimated from the stabilized voltammogram.

Assuming that the nickel oxide layer was homogeneously distributed over the entire substrate, the value of $\langle L \rangle$, the average film thickness, was estimated from the ratio

$$\langle L \rangle = \frac{q_r M}{F\delta} \tag{2}$$

where q_r is the apparent electroreduction charge density referred to the WE geometric area, and M and δ are the molecular weight, and the average specific gravity of the oxide layer, respectively. Thus, considering that the α-$Ni(OH)_2.2/3H_2O$ stoichiometry is applicable to the oxide layer produced by the SWP treatment, and $\delta = 2.5\,g\,cm^{-3}$ [21], it follows that

$$\langle L \rangle = 4.33\,q_r \tag{3}$$

where q_r is expressed in $mC\,cm^{-2}$ and $\langle L \rangle$ in nm.

Electrochemical data were complemented with X-ray diffractometry, infrared spectroscopy, and scanning electron microscopy data.

3. Results

3.1. *Voltammetric data*

A typical voltammogram of polycrystalline nickel in aqueous 1 M NaOH at 30 °C run at 0.1 V s^{-1} (blank) (Fig. 1(a)) shows a pair of peaks in the range 1.3–1.5 V just preceding the OER potential range. This pair of peaks is related to the Ni(II)/Ni(III) redox reactions at the nickel oxide layer. A similar run made after the application of the SWP for $E_l = -1.0$ V, $E_u = 1.0$ V, $f = 2.0$ kHz and $t = 30$ s, resulted in a voltammogram (Fig. 1(b)) comprising a charge greater by a factor of about 150 than that of the blank, and a broader conjugated pair of current peaks.

The voltammetric charge increases with n, the number of potential sweeps up to a certain value $n = n_s$. Afterwards, it is almost constant. The value of n_s depends on the amount of oxide layer formed on the WE, as well as on the potential sweep characteristics. By holding the potential at $E_p = 1.6$ V for $t = t_p$ ($0 \text{ s} \leqslant t_p \leqslant 150$ s) after the SWP treatment, an increase in the voltammetric charge which depends on both E_p and t_p can be observed (Fig. 1(c)). This increase can be related to the rather low rate of conversion from Ni(II) into Ni(III) in the active material, as has been described for chemically precipitated $Ni(OH)_2$ in the same solution [21, 22]. In contrast, the voltammetric response of the nickel oxide layers after a potential holding at 0 V shows a large increase in the electro-oxidation voltammetric charge as compared to that resulting from the previous potential sweep in the positive direction (Fig. 1(d)). According to these results, the conversion from Ni(III) into Ni(II) should also be considered as a rather slow process.

In conclusion, the general electrochemical behaviour of the nickel oxide layer produced by the SWP treatment is somewhat similar to that of chemically prepared thick nickel oxide layers used for batteries [10–12, 22–27].

3.2. *The dependence of q_r and R on the SWP characteristics*

The optimal SWP characteristics for producing thick hydrous nickel oxide layers depend on the NaOH concentration in the solution. The q_r against E_u plot resulting from the following preparation conditions, $-1.0 \text{ V} \leqslant E_l \leqslant -1.3 \text{ V}$ and $1.6 \text{ kHz} \leqslant f \leqslant 2 \text{ kHz}$ (Fig. 2), exhibits a single maximum charge density value (q_{rM}) in the range $1.0 \text{ V} \leqslant E_u \leqslant 1.2 \text{ V}$ for aqueous 3 M NaOH (Fig. 2(c)), and two charge density maxima (q_{rM1} and q_{rM2}) in the range $1.0 \text{ V} \leqslant E_u \leqslant 1.1 \text{ V}$ and $1.6 \text{ V} \leqslant E_u \leqslant 1.7 \text{ V}$, respectively, for both aqueous 0.1 M and 1 M NaOH (Fig.

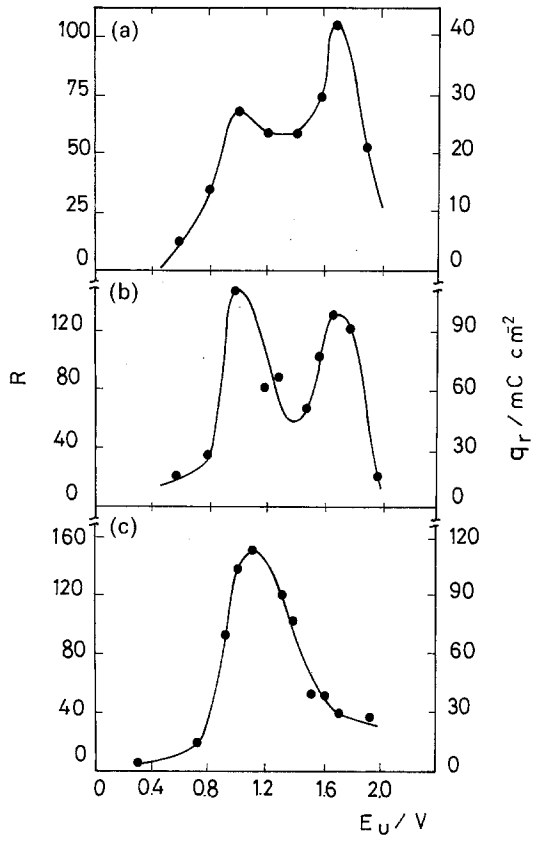

Fig. 2. Dependence of q_r and R on E_u. (a) 0.1 M NaOH; $E_l = -1.3$ V, $f = 1.66$ kHz; $t = 60$ s. (b) 1 M NaOH; $E_l = -1.2$ V, $f = 2.0$ kHz; $t = 30$ s. (c) 3 M NaOH; $E_l = -1.0$ V, $f = 2.0$ kHz; $t = 5$ s. $T = 30$ °C.

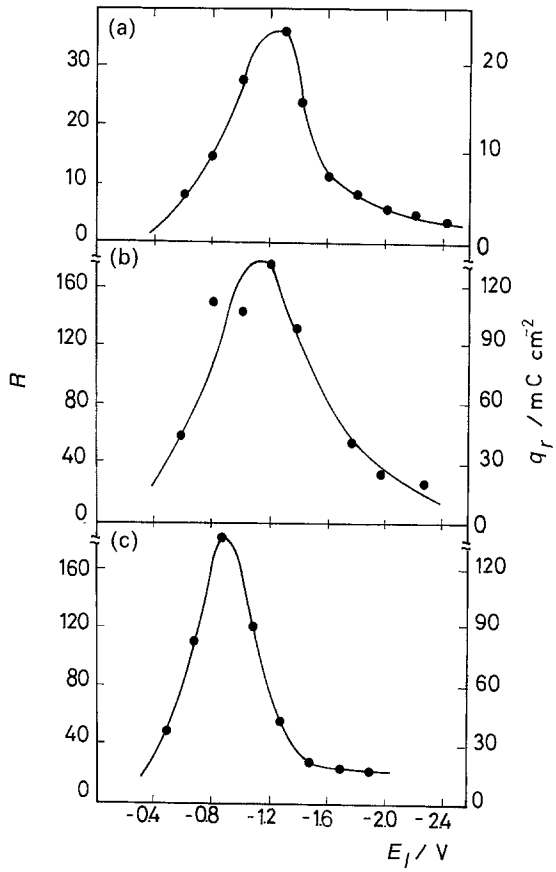

Fig. 3. Dependence of q_r and R on E_l. (a) 0.1 M NaOH; $E_u = 1.0$ V, $f = 1.66$ kHz; $t = 60$ s. (b) 1 M NaOH; $E_u = 1.0$ V, $f = 2.0$ kHz; $t = 30$ s. (c) 3 M NaOH; $E_u = 1.0$ V, $f = 2.0$ kHz; $t = 5$ s. $T = 30$ °C.

2(a) and (b)). The following order of the q_{rM} values can be established: q_{rM} (3 M NaOH) > q_{rM1} (1 M NaOH) > q_{rM1} (0.1 M NaOH) and (q_{rM1}/q_{rM2}) (1 M NaOH) > (q_{rM1}/q_{rM2}) (0.1 M NaOH). The range of E_u, where the contribution of q_{rM2} can be noticed, coincides with the potential range where the voltammetric electrooxidation current peaks related to the Ni(II) to Ni(III) reaction are observed (Fig. 1). Conversely, the contribution of q_{rM1} appears in a range of E_u which coincides with the range of potential where the electroformation of the nickel oxide layer involves the participation of Ni(II) species only. As it has been reported elsewhere [2, 3], the electroformation and electroreduction of Ni(II) species occur at low potentials where the growth of a thick oxide layer of nickel in alkaline solution takes place.

The q_r against E_l plots (Fig. 3) show a bell-shaped curve for all solutions, although the value of q_{rM} increases and shifts positively as the NaOH solution concentration is increased, the corresponding current peak being narrower. In all solutions, for the optimal SWP conditions, the dependence of q_r on t yields a curve approaching a linear portion for $t \to 0$, and a limiting value for $t \to \infty$ (Fig. 4). Furthermore, the initial slope increases almost linearly with the NaOH concentration.

For $-1.0\,V \leqslant E_l \leqslant -1.3\,V$ and $E_u = 1.0\,V$, the q_r against f plot (Fig. 5) exhibits a single maximum charge density value in 1 M and 3 M NaOH at

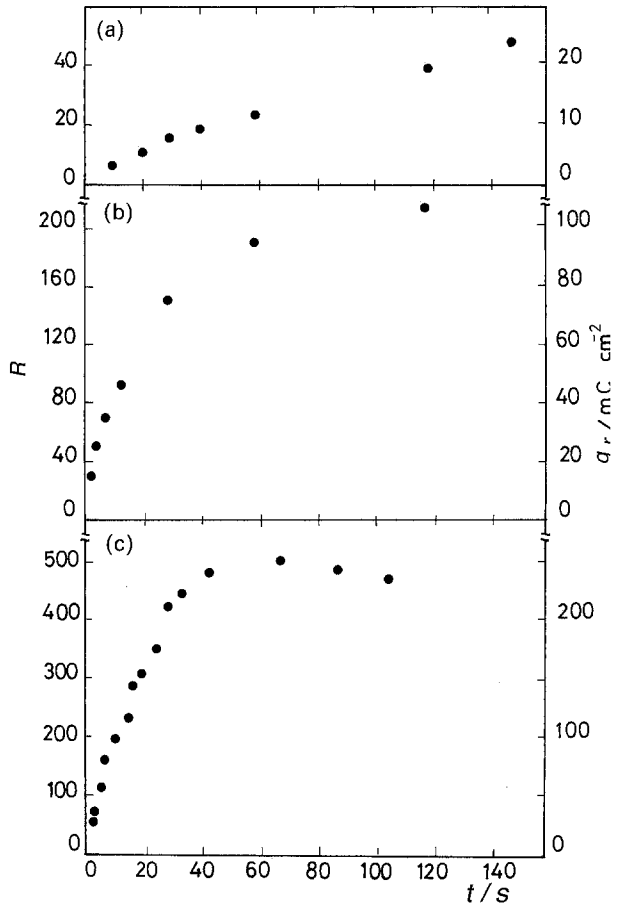

Fig. 4. Dependence of q_r and R on t. (a) 0.1 M NaOH; $E_u = 1.3\,V$, $E_l = -1.0\,V$; $f = 2.5\,kHz$ (b) 1 M NaOH; $E_u = 1.0\,V$, $E_l = -1.2\,V$, $f = 2.0\,kHz$. (c) 3 M NaOH; $E_u = 1.0\,V$, $E_l = -1.0\,V$, $f = 2.0\,kHz$. $T = 30\,°C$.

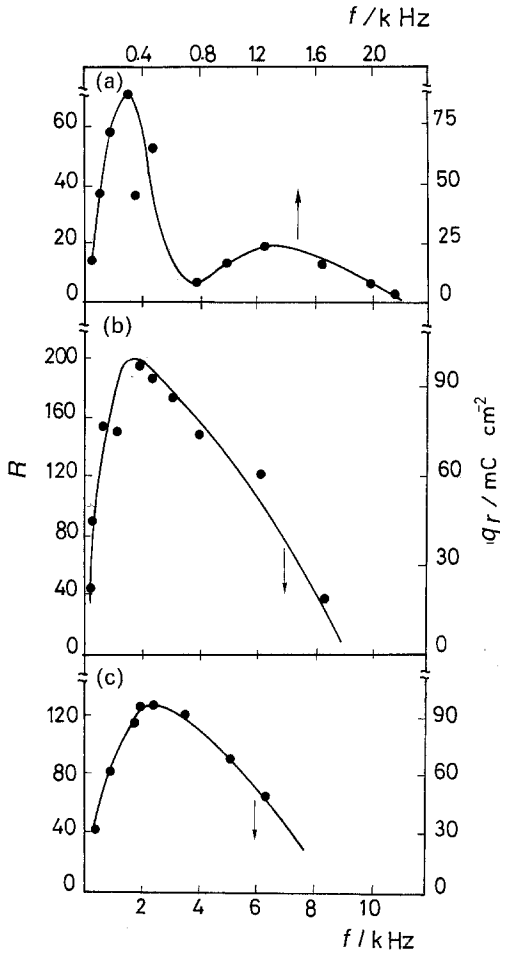

Fig. 5. Dependence of q_r and R on f. (a) 0.1 M NaOH; $E_l = -1.3\,V$, $E_u = 1.0\,V$, $t = 60\,s$. (b) 1 M NaOH; $E_l = -1.2\,V$, $E_u = 1.0\,V$; $t = 30\,s$. (c) 3 M NaOH; $E_l = -1.0\,V$, $E_u = 1.0\,V$; $t = 5\,s$. $T = 30\,°C$.

$f \simeq 2\,kHz$, and two charge density maxima in 0.1 M NaOH at $f = 0.35\,kHz$ and $f = 1.3\,kHz$.

The q_r against τ_u/τ_l plot (Fig. 6) provides information about the influence of the symmetry of the SWP routine on the overall process. For aqueous 1 M NaOH, the values of q_{rM1} and q_{rM2} appear at $\tau_u/\tau_l = 1$ and $\tau_u/\tau_l = 1.4$, respectively. Conversely,

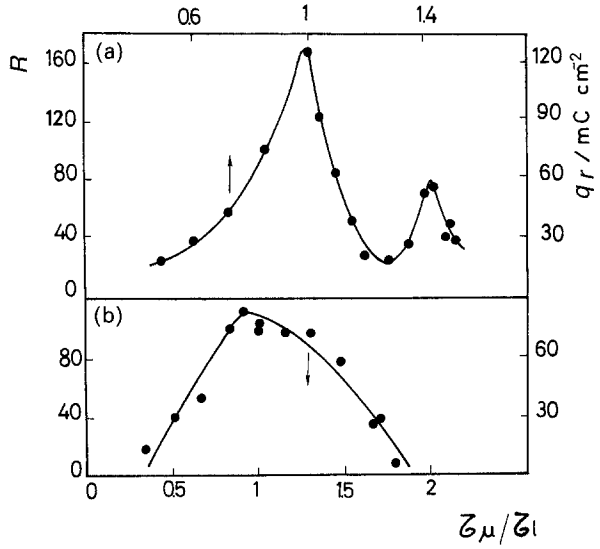

Fig. 6. Dependence of q_r and R on τ_u. (a) 1 M NaOH; $E_u = 1.0\,V$, $E_l = -1.2\,V$, $f = 2.0\,kHz$; $t = 30\,s$. (b) 3 M NaOH; $E_u = 1.0\,V$, $E_l = -1.0\,V$, $f = 1.66\,kHz$; $t = 5\,s$. $T = 30\,°C$.

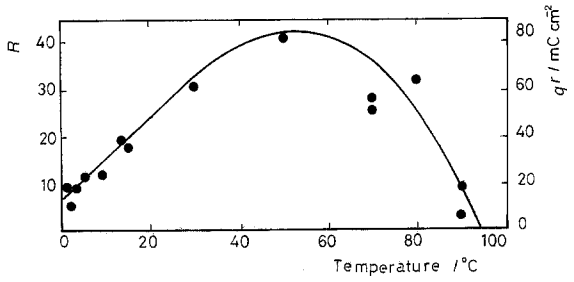

Fig. 7. Dependence on q_r and R on the temperature employed in the SWP treatment. 0.1 M NaOH; $E_l = -1.6$ V, $E_u = 1.7$ V, $f = 2.0$ kHz; $t = 60$ s.

for aqueous 3 M NaOH, the value of q_{rM} is observed at $\tau_u/\tau_l = 1$.

In contrast, the value of R increases almost linearly with the temperatures in the range 0–35 °C (Fig. 7), reaching a maximum at 50 °C. Then, it drops to nearly 1 at about 90 °C. These results are in agreement with those reported earlier in the literature [2].

3.3. *Stability of hydrous nickel oxide layers obtained by the SWP treatment*

The stability of hydrous nickel oxide layers produced by the SWP treatment in aqueous 1 M NaOH at 30 °C for $E_l = -1.7$ V, $E_u = 1.0$ V and $f = 2.0$ kHz, was tested by subjecting the hydrous nickel oxide layers to an ORC treatment between 0 and 1.6 V at 0.02 V s^{-1} for a time t_c (Fig. 8(a)). The value of q_r resulting from these voltammograms goes down almost linearly with t_c. The value of the rate of decay increases with the initial amount of accumulated oxide (Fig. 8(b)). This decrease is accompanied by the appearance of a multiplicity of voltammetric electroreduction current peaks (Fig. 9(a)), and a change in the height ratio of the anodic to cathodic current peak, the peak located more positively being predominant as q_r decreases. Furthermore, as

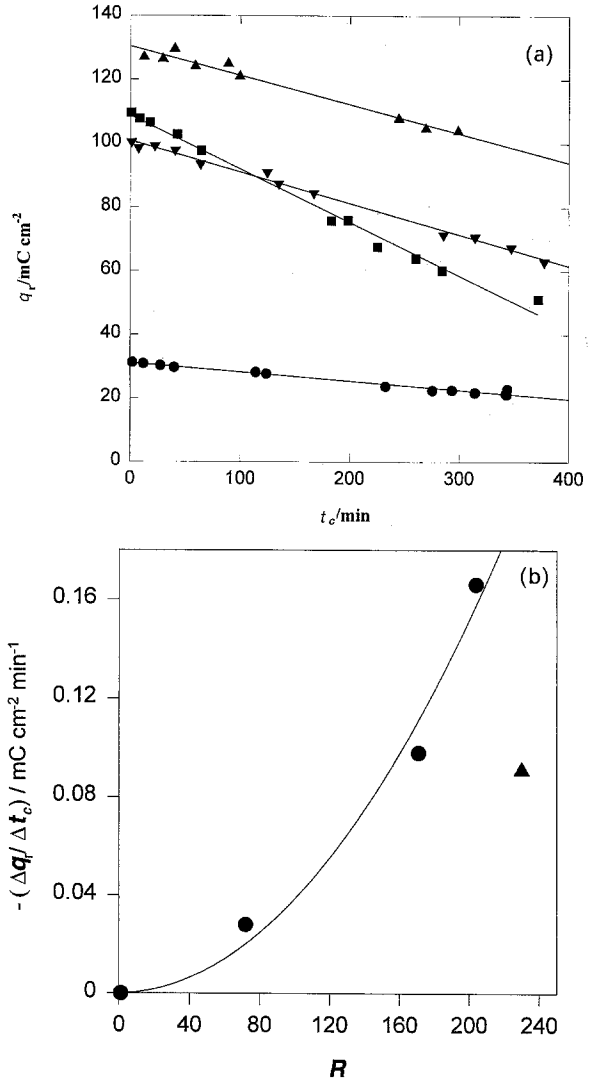

Fig. 8. (a) q_r against potential cycling time (t_c) at 0.02 V s^{-1} between 0 and 1.6 V for SWP prepared nickel oxide electrodes with different values of R. (●) $R = 72$; (▼) $R = 171$, and (■) $R = 204$. SWP treatment conditions: $E_l = -1.7$ V, $E_u = 1.0$ V, $f = 2.0$ kHz; 1 M NaOH, $T = 30$ °C. (▲) nickel oxide electrode of $R = 230$ prepared in 1 M LiOH, $T = 30$ °C, by setting $E_l = -1.0$ V, $E_u = 1.2$ V, $f = 1.25$ kHz and $t = 30$ s. (b) Dependence of $-\Delta q_r/\Delta t_c$ on R for nickel oxide electrodes prepared by the SWP treatment as indicated for Fig. 8(a).

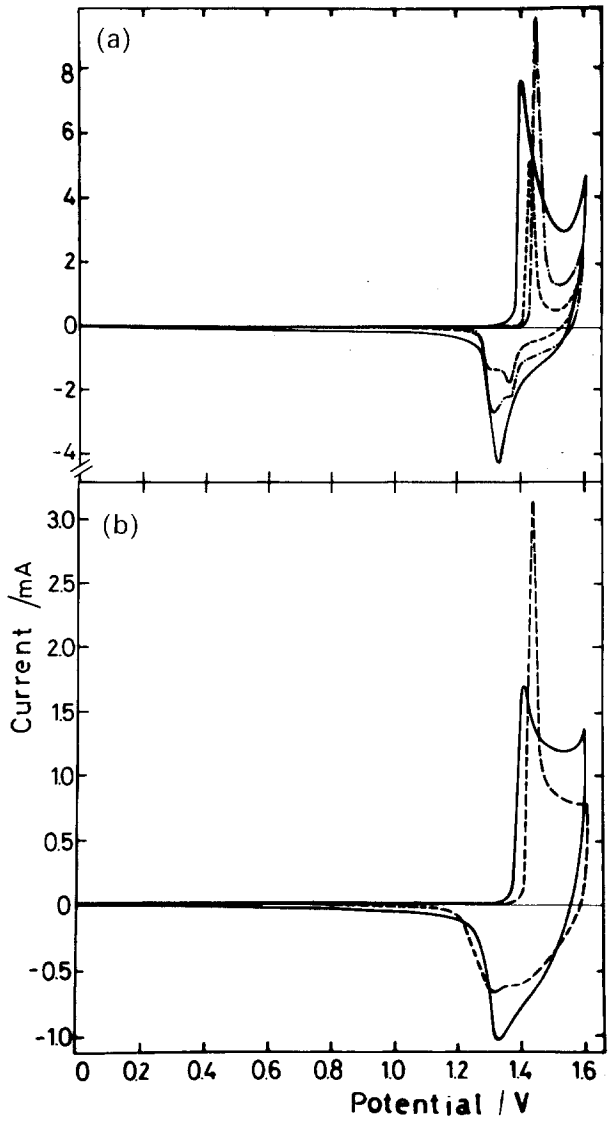

Fig. 9. (a) Voltammograms for a SWP prepared nickel oxide electrode subjected to ORC at 0.02 V s^{-1} between 0 and 1.6 V in 1 M NaOH, $T = 30$ °C. SWP treatment conditions in 1 M NaOH are the same as those indicated in Fig. 8; $R = 204$; (——) 2nd cycle; (– · –) 130th cycle; (– –) 180th cycle. (b) Voltammograms for a SWP prepared nickel oxide electrode subjected to ORC at 0.02 V s^{-1} between 0 and 1.6 V in 1 M LiOH at 30 °C. SWP treatment conditions in 1 M LiOH are the same as those indicated in Fig. 8; (——) 2nd cycle; (– –) 90th cycle.

$t_c \rightarrow \infty$, the overall voltammogram approaches that illustrated in Fig. 1(a).

3.4. *Voltammetry in aqueous 1 M LiOH*

In general, when foreign cations are present in the nickel hydroxide structure the activity of water at interplanar regions diminishes [25, 28, 29]. This effect depends on the cation charge and size. Thus, the insertion of Li^+ ions into the nickel hydroxide structure makes β-NiOOH more stable and favours the corresponding electroreduction process. To learn further aspects of this process, hydrous nickel oxide electrodes were prepared by SWP treatment in aqueous 1 M LiOH at 30 °C, by setting $E_l = -1.0$ V, $E_u = 1.2$ V, $f = 1.25$ kHz and $t = 30$ s. The hydrous nickel oxide electrode was subsequently subjected to an ORC treatment between 0 and 1.6 V at 0.02 V s^{-1} for 5 h. In this case, the decrease in q_r with t_c is much lower than that observed in aqueous 1 M NaOH for hydrous nickel oxide electrodes of similar R values (Fig. 8).

Voltammograms resulting from hydrous nickel oxide electrodes subjected to an ORC treatment at 0.02 V s^{-1} in 1 M LiOH at 30 °C (Fig. 9(b)), show that the anodic peak becomes sharper and the splitting of the cathodic peak is less remarkable than in aqueous 1 M NaOH, as t_c increases.

3.5 *Oxygen evolution reaction polarization curves*

The oxygen evolution reaction (OER) quasi-stationary polarization curves were run at 2×10^{-4} V s^{-1} in 1 M NaOH at 30 °C using either an untreated nickel electrode or SWP-treated nickel electrodes in 1 M NaOH at 30 °C. These curves were obtained immediately after the working electrode had been subjected to a potential cycling between 0.05 and 1.55 V at 0.1 V s^{-1} for about 15 min to attain a stable voltammetric response. In all cases, the values of the current density were referred to the geometric electrode area (Fig. 10). At constant potential, the anodic current density related those SWP-treated nickel electrodes is greater than that of the untreated nickel. Besides, the increase in the OER catalytic activity for SWP treated electrodes correlates with the increase in the working electrode active surface area.

3.6. *SEM micrographs*

SEM micrographs of fresh hydrous nickel oxide layers prepared by the SWP treatment show a gel-like structure (Fig. 11(a)). No crystalline texture can be distinguished, in agreement with X-ray diffractograms (Section 3.7). Following an ORC treatment between 0 and 1.6 V at 0.02 V s^{-1} for $t = 225$ min, in either aqueous 1 M NaOH or 1 M LiOH, a rather regular shrinked mosaic-like structure [30] can be observed (Fig. 11(b)).

3.7. *X-ray difractometry*

X-ray diffractograms of hydrous nickel oxide electrodes prepared in aqueous 1 M NaOH setting either $E_l = -1.0$ V, $E_u = 1.0$ V; $f = 2.0$ kHz, $t = 1$ min or $E_l = -1.6$ V, $E_u = 1.7$ V; $f = 2.0$ kHz, $t = 1$ min (Fig. 12(a) and (b)) show peaks of bulk nickel at 52.3° and 45.2° which correspond to reflections at the (2 0 0) and (1 1 1) planes, respectively, but no peak related to nickel hydroxide can be observed. After drying, the same material exhibits a very poor degree of crystallinity.

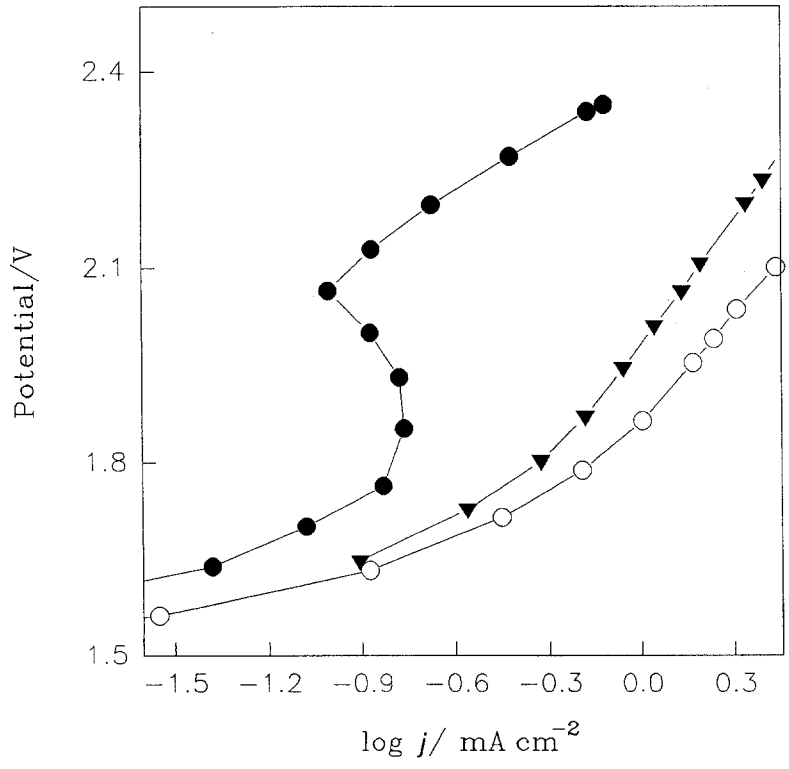

Fig. 10. OER polarization curves for differently prepared nickel electrodes in 1 M NaOH at 30 °C. Data obtained at 2×10^{-4} V s^{-1}. Untreated polycrystalline nickel electrode (●). SWP treated nickel electrodes: (▼) $R = 28$, and (○) $R = 110$.

For the sake of comparison, diffractograms of differently prepared nickel oxide powders were also obtained. Thus, diffractograms resulting from nickel hydroxide powders, precipitated from an aqueous $NiCl_2$ solution (Fig. 12(c)), show peaks that are typical of a crystalline substance involving reflections at the (1 1 0), (1 0 1), (1 0 0) and (0 0 1) planes [31, 32]. Likewise, nickel oxide samples prepared in aqueous 1 M NaOH by setting either $E_l = -1.5$ V, $E_u = 1.2$ V, and $f = 2.5$ kHz, or $E_l = -1.6$ V, $E_u = 1.7$ V, and $f = 2.5$ kHz, and stored for 48 h at 80 °C, provide X-ray diffractograms which exhibit incipient nickel hydroxide peaks (Fig. 12(d) and (e)). The X-ray diffractograms of these samples, kept for three months in aqueous 1 M NaOH (Fig. 12(f)), tend to exhibit the features of a diffractogram resulting from chemically prepared nickel oxide.

These results show that fresh hydrous nickel oxide layers produced by the SWP technique can be considered as largely amorphous [32–34]. However, a change in the structure and morphology of these layers takes place when the electrodes are kept in aqueous NaOH under open circuit conditions. Furthermore, the evolution of the voltammogram resulting from SWP-prepared hydrous nickel oxide electrodes and kept in contact with aqueous NaOH is comparable to that recently described for hydrous cobalt oxide [6–8].

3.8. *Infrared spectroscopy data*

Infrared spectra of hydrous nickel oxide prepared either at $E_l = -1.5$ V, $E_u = 1.2$ V, $f = 2.5$ kHz and $t = 6$ h (specimen I), or $E_l = -1.6$ V, $E_u = 1.7$ V, $f = 2.5$ kHz and $t = 6$ h (specimen II) were obtained. After the SWP treatment, a greenish product is formed on specimen I, whereas a black substance appears on specimen II. Both products were dried at 100 °C to obtain their infrared spectrum (Fig. 13(a) and (b)). Assignments of significant absorption bands have been given elsewhere [35–41]. The band at 3640 cm^{-1} related to free OH stretching vibration characterizes $Ni(OH)_2$ [36, 37]. The band at 3434 cm^{-1} has been assigned to either an adsorbed OH stretching mode or to the vibration of OH groups involved in hydrogen bonding in NiOOH [39–41].

For the sake of comparison, the infrared spectrum of nickel oxide precipitated by adding aqueous NaOH to $NiCl_2$, filtered, and vacuum dried at 100 °C for 30 h was also obtained (Fig. 13(c)) [32, 34]. It exhibits $Ni(OH)_2$ as the predominant species. Analogously, Ni oxide prepared as indicated in [34], subsequently oxidized with bromine, filtered and vacuum dried gives a Ni(III) oxide infrared spectrum (Fig. 13(d)) [32, 34].

Accordingly, it can be concluded from infrared data that nickel oxide layers prepared by the SWP technique can be considered as a mixture of Ni(II) and

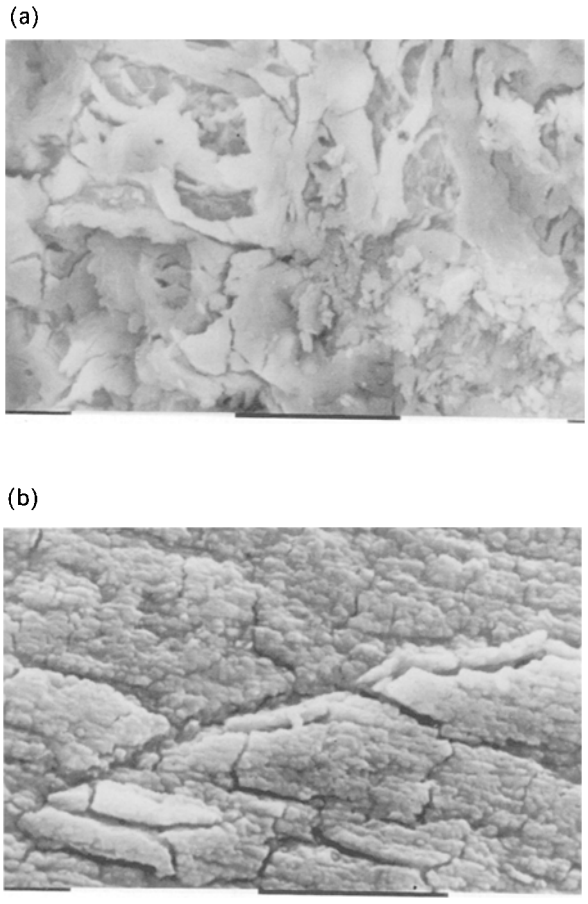

Fig. 11. SEM micrographs. Scale: 10 μm. (a) Nickel oxide layer produced in 1 M NaOH at 30 °C by setting $E_l = -1.0$ V, $E_u = 1.0$ V, $f = 2.0$ kHz, $t = 45$ s. (b) Same specimen after a 225 min ORC treatment between 0 and 1.6 V at 0.02 V s^{-1}.

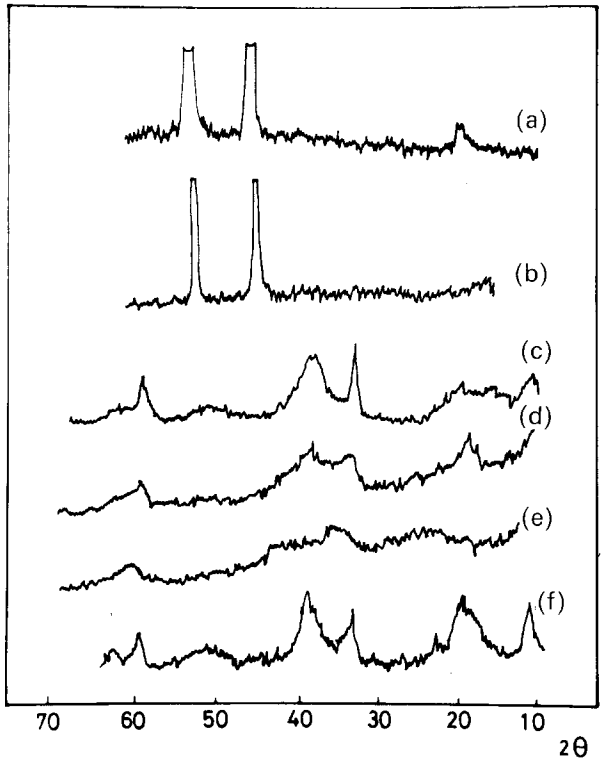

Fig. 12. X-ray diffractograms of differently prepared nickel oxide samples. (a) Sample prepared by applying the SWP technique, $E_l = -1.0$ V, $E_u = 1.0$ V, $f = 2.0$ kHz, $t = 60$ s, 1 M NaOH, 30 °C. (b) The same as in (a) except for $E_l = -1.6$ V and $E_u = 1.7$ V. (c) Sample prepared by precipitation from $NiCl_2$ and NaOH solutions. (d) SWP prepared sample, $E_l = -1.5$ V, $E_u = 1.2$ V, $f = 2.5$ kHz, $t = 60$ s, 1 M NaOH, 30 °C and further heated at 80 °C for 48 h. (e) The same as in (d) except for $E_l = -1.6$ V, $E_u = 1.7$ V. (f) Same as in (d) after a three month ripening in 1 M NaOH.

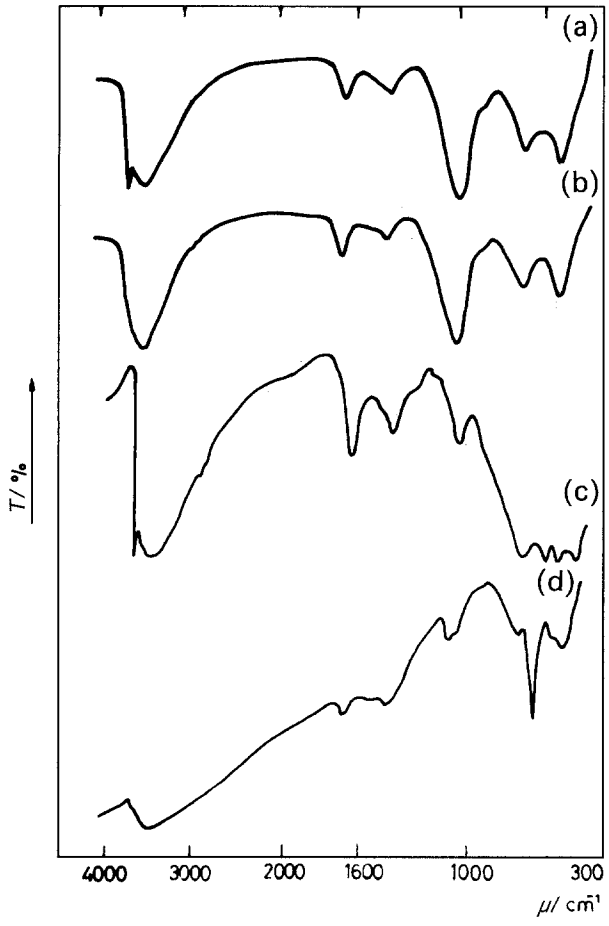

Fig 13. Infrared spectra of differently prepared nickel oxide samples (a) SWP prepared sample, $E_l = -1.5$ V, $E_u = 1.2$ V, $f = 2.5$ kHz, $t = 6$ h, 1 M NaOH, $T = 30$ °C. (b) Same as in (a) but $E_l = -1.6$ V, $E_u = 1.7$ V. (c) Sample prepared by precipitation from $NiCl_2$ and NaOH solutions. (d) Same as in (c) with further chemical oxidation by bromine addition.

Ni(III) species, although Ni(III) species predominate for specimen II.

4. Discussion

4.1. *Formation of hydrous nickel oxide electrodes by the SWP treatment*

The electroformation of hydrous nickel oxide by the SWP technique depends on the characteristics of the periodic potential routine, as earlier established [5], and also on the solution composition. It is clear that the value of E_l related to q_{rM} lies in the potential range where the simultaneous HER and Ni(II) electrodeposition take place, leading in part to the precipitation of $Ni(OH)_2$ [42, 43]. The overall process becomes directly comparable to that already described for SWP treated cobalt electrodes in alkaline solution [6–8].

The dependence of q_r on E_u (Fig. 2) indicates that the values of q_{rM1} and q_{rM2} in aqueous 1 M and 0.1 M NaOH are associated with the E_u values which are located in the potential range where $Ni(OH)_2$ and NiOOH species, respectively, are formed, as concluded from the analysis of infrared spectra described in Section 3.8. The single q_{rM} maximum in aqueous 3 M NaOH appears in the potential range where only electrochemical reactions related to $Ni(OH)_2$ are thermodynamically possible [43]. Therefore, the amount of active species produced by SWP is independent of the oxidation state of those nickel species produced anodically.

In aqueous 0.1 M and 1.0 M NaOH, the appearance of a thick hydrous nickel oxide layer can be explained by the following overall reactions:

$$Ni + 2OH^- = Ni(OH)_2^* + 2e^- \qquad (4a)$$

and

$$Ni(OH)_2^* + OH^- = NiOOH^* + H_2O + e^- \qquad (5a)$$

Reactions 4(a) and 5(a) can be related to q_{rM1} and q_{rM2}, respectively. Asterisks stand for 'non-aged' species [5] produced in the relatively short anodic half-cycle time. Furthermore, at sufficiently positive potentials, the following process competes with Reaction 5(a):

$$Ni(OH)_2^* + 2OH^- = NiO_2^- + 2H_2O + e^- \qquad (5b)$$

yielding soluble nickel–anionic species. According to thermodynamics, Reaction 5(b) should occur at above 1.6 V, and is favoured by increasing the solution pH [42]. Therefore, owing to the contribution of Reaction 5(b), which prevails in aqueous 3 M NaOH instead of Reaction 5(a), no second maximum value can be observed in the q_r against E_u plot for this high NaOH concentration. This conclusion is supported by the higher yield of soluble nickel species produced during the SWP treatment on increasing the NaOH concentration when E_u exceeds 1.6 V [5].

The frequency dependence of q_r in aqueous 1 M and 3 M NaOH is rather similar (Fig. 5) as it goes through a single q_{rM} for $f \simeq 2$ kHz, whereas two maxima, q_{rM1} at $f \simeq 0.35$ kHz and q_{rM2} at $f \simeq 1.3$ kHz, appear at 0.1 M NaOH. The frequency related to q_{rM2} at $f \simeq 1.3$ kHz can be related to q_{rM} for more concentrated solutions. The appearance of q_{rM1} at $f \simeq 0.35$ kHz in aqueous 0.1 M NaOH suggests that, under these conditions, Reaction 5(b) is nearly suppressed and then, oxide layer formation involves again a dominating participation of Reactions 4(a) and 5(a) in the overall process. Therefore the competition among Reactions 4(a), 5(a) and 5(b) provides a reasonable explanation for the influence of the solution composition and characteristics of the potential routine on the formation of the hydrous nickel oxide layers on nickel in alkaline solutions. In fact the rate and yield of those reactions depend on E_u, E_l, τ_u, τ_l and the solution composition. Therefore, it is possible to select the optimal conditions to produce hydrous nickel oxide electrodes of different thicknesses.

For the OER those hydrous nickel oxide electrodes produced by the SWP treatment at constant potential can hold higher current densities than the untreated nickel electrode. This enhancement in the catalytic activity for OER can be related, as previously reported by Burke *et al.* [3], to the hydrous structure of metal oxide layers produced by the application of periodic potential routines (see Sections 3.7 and 3.8).

4.2. *Dependence of the charge storage capacity on ORC*

The decrease in the charge storage capacity of hydrous nickel oxide electrodes on ORC fits closely a linear q_r against t_c relationship (Fig. 8(a)). The charge storage capacity decay follows a zero order rate law in all solutions. At constant temperature, the apparent zero order rate constant $k' = -\Delta q_r/\Delta t_c$, depends on R and the solution composition (Fig. 8(b)). Thus, for aqueous 1 M NaOH, the value of k' increases from 0.028 to $0.163\,mC\,cm^{-2}\,min^{-1}$ when the value of R is changed from 72 to 204. Furthermore, for $204 \leqslant R \leqslant 230$, k' decreases from $0.163\,mC\,cm^{-2}\,min^{-1}$ for aqueous 1 M NaOH to $0.092\,mC\,cm^{-2}\,min^{-1}$ for aqueous 1 M LiOH. These results indicate that during each ORC a certain amount of material becomes inactive, this amount of inactive material being proportional to the number of ORCs. The conversion from active into inactive material is known to be a slow process which can be followed through voltammetric sampling [19, 20], where it appears that the complex mixtures of hydrous nickel oxides initially formed change into chemically defined species such as α-$Ni(OH)_2$, β-$Ni(OH)_2$, β-NiOOH and γ-NiOOH, which are usually assigned to nickel oxide electrodes of technical interest.

The incorporation of Li^+ ions into the hydrous nickel hydroxide matrix also makes this type of electrode more efficient for long-term charging-discharging cycles, in agreement with earlier results [25, 28, 29].

4.3. *Influence of temperature*

The amount of hydrous nickel oxide accumulated during the SWP treatment, as evaluated by R, increases with T until a certain critical temperature ($T_c \approx 50\,°C$) is reached and then it decreases approaching zero for $T \approx 95\,°C$ (Fig. 7). The increase in R with T resulting from $T < T_c$ obeys the linear q_r against T relationship, as earlier reported in the literature [2]. This fact can be explained by the increase in the rate of Reactions 4(a), 5(a) and 5(b) with temperature, and a negligible contribution of those side reactions leading to the conversion from active into inactive electrode material. However, the decrease in R with T, which is observed for $T > T_c$ indicates that in this case there is a competition between hydrous nickel oxide electroformation and ageing processes producing inactive materials. In contrast with these materials, fresh hydrous nickel oxide layers produced by applying the SWP treatment exhibit amorphous characteristics and a rather large content of water [3, 5], as concluded from X-ray diffractometry and infrared spectroscopy data. Furthermore, the temperature increase diminishes the adherence of the oxide layer to the base electrode, favouring the formation of a powder-like poorly adherent inactive product. Therefore, a greater efficiency for the production of hydrous nickel oxide electrodes is expected in the low range of temperature for $T < T_c$.

Acknowledgements

This work was financial supported by the Consejo Nacional de Investigaciones Científicas y Técnicas of Argentina, the Comisión de Investigaciones Científicas of Provincia de Buenos Aires, and the Regional Program for the Scientific and Technological Development of the Organization of American States.

References

[1] A. C. Chialvo, W. E. Triaca and A. J. Arvia, *J. Electroanal. Chem.* **146** (1983) 93.
[2] L. D. Burke and T. A. M. Twomey, *ibid.* **162** (1984) 101.
[3] L. D. Burke and M. E. G. Lyons, *in* 'Modern Aspects of Electrochemistry', Vol. 18 (edited by R. E. White, J. O'M. Bockris and B. E. Conway), Plenum Press, New York (1986) p. 169.
[4] A. J. Arvia, R. C. Salvarezza and W. E. Triaca, *Electrochim. Acta* **34** (1989) 1057.
[5] A. Visintin, A. C. Chialvo, W. E. Triaca and A. J. Arvia, *J. Electroanal. Chem.* **225** (1987) 227.
[6] T. Kessler, A. Visintin, M. R. de Chialvo, W. E. Triaca and A. J. Arvia, *ibid.* **261** (1988) 315.
[7] M. R. Gennero de Chialvo and A. C. Chialvo, *Electrochim. Acta* **33** (1988) 825.
[8] M. R. de Chialvo, T. Kessler, A. Visintin, W. E. Triaca and A. J. Arvia, *J. Appl. Electrochem.* **21** (1991) 516.
[9] D. L. Britton, *in* Proceedings of the fourth international rechargeable battery seminar (edited by S. P. Wolsky and N. Marincic), Deerfield Beach, FA (1992) p. 158.
[10] J. D. Dunlop, *in* 'Handbook of Batteries & Fuel Cell', (edited by D. Linden), McGraw-Hill, New York (1984) chapter 22, p. 1.
[11] M. Z. A. Munshi, A. C. C. Tseung and J. Parker, *J. Appl. Electrochem.* **15** (1985) 711.
[12] J. J. Smithrick, *in* 'Modern Battery Technology' (edited by C. D. S. Tuck), Ellis Horwood, Chichester, UK (1991) p. 472.
[13] M. J. Natan, D. Bélanger, M. K. Carpenter and M. S. Wrighton, *J. Phys. Chem.* **91** (1987) 1834.
[14] M. K. Carpenter and D. A. Corrigan, *J. Electrochem. Soc.* **136** (1989) 1022.
[15] H. J. Schäfer, *Top Curr. Chem.* **142** (1987) 101.
[16] D. A. Corrigan, *J. Electrochem. Soc.* **134** (1987) 377.
[17] H. Bode, K. Dehmelt and J. Witte, *Electrochim. Acta.* **11** (1966) 1079.
[18] R. Barnard, C. F. Randell and F. L. Tye, *in* Proceedings of the symposium on the nickel electrode (edited by R. G. Gunther and S. Gross), The Electrochemical Society, Pennington, NJ (1982) p. 69.
[19] R. S. Schrebler Guzmán, J. R. Vilche and A. J. Arvia, *J. Appl. Electrochem.* **9** (1979) 321.
[20] *Idem, J. Electrochem. Soc.* **125** (1978) 1578.
[21] R. E. Carbonio, V. A. Macagno, M. C. Giordano, J. R. Vilche and A. J. Arvia, *ibid.* **129** (1982) 983.
[22] C. R. Dyer, *in* Proceedings of the symposium on the nickel electrode, op. cit. [18], p. 119.
[23] D. N. Buckley and L. D. Burke, *Faraday Trans. I* **72** (1976) 2431.
[24] K. Manandhar and D. Pletcher, *J. Appl. Electrochem.* **9** (1979) 707.
[25] V. A. Volynskii and Yu. N. Chernykh. *Elektrokhimiya* **13** (1979) 1874.
[26] D. M. Mac Arthur, *J. Electrochem. Soc.* **117** (1980) 422.
[27] S. H. Glarum and J. H. Marshall, *ibid.* **129** (1982) 535.
[28] E. A. Kaminskaya, N. Yu. Uflyand and S. A. Rozentsveig, *Elektrokhimiya* **7** (1971) 1839.
[29] J. L. Weininger, *in* Proceedings of the symposium on the nickel electrode *op. cit.* [18], p. 1.
[30] A. Delahaye-Vidal, B. Beaudoin and M. Figlarz, *Reactivity Solids* **2** (1986) 223.
[31] R. S. McEwen, *J. Phys. Chem.* **75** (1971) 1782.

[32] H. Bode, K. Dehmelt and J. Witte, *Z. Anorg. Allg. Chem.* **366** (1969) 1.
[33] R. Barnard, C. F. Randell and F. L. Tye, *Power Sources* (edited by J. Thompson), vol. 8, Academic Press, London (1981) p. 401.
[34] H. Bartl, H. Bode, G. Sterr and J. Witte, *Electrochim. Acta* **16** (1971) 615.
[35] J. F. Jackovitz, *in* Proceedings of the symposium on the nickel electrode, *op. cit.* [18], p. 49.
[36] F. P. Kober, *J. Electrochem. Soc.* **112** (1965) 1064.
[37] *Idem, ibid.* **114** (1967) 2154.
[38] S. A. Aleshkevich, E. E. Gol'teuzen, V. P. Morozov and L. N. Sagoyan, *Elektrokhimiya* **4** (1968) 590.
[39] I. S. Shamina, O. G. Malandin, S. M. Rakhovskaya and L. A. Vereshchagina, *ibid* **10** (1974) 1745.
[40] O. G. Malandin, S. M. Rakhovskaya, A. V. Vasev, L. A. Vereshchagina and G. V. Suchkova, *ibid.* **16** (1980) 1041.
[41] O. G. Malandin and B. B. Ezhov, Russ. *J. Electrochem.* **31** (1995) 368.
[42] D. M. MacArthur, *in* 'Power Sources' (edited by D. H. Collins) vol. 3, Oriel Press, Newcastle-upon-Tyne (1971) p. 91.
[43] A. J. Bard, R. Parsons and J. Jordan (eds), 'Standard Potentials in Aqueous Solutions', Marcel Dekker, New York (1985) p. 329.